## ACKNOWLEDGMENTS

We thank Matthew Johnson, CNMT; Mansoor Farooki, MD; Claude Margouleff, MS; T. Chaly, PhD; J.R. Dahl, PhD; and R. Matachierri, cyclotron engineer, for assistance.

## REFERENCES

1. Israel O, Front D, Epelbaum R, et al. Residual mass and negative gallium scintigraphy in treated lymphoma. *J Nucl Med* 1990;31:365–368.
2. Paul R. Comparison of $^{18}$F-2-fluorodeoxyglucose and $^{67}$Ga citrate imaging for detection of lymphoma. *J Nucl Med* 1987;28:288–292.
3. Okada J, Yoshikawa K, Itami M, et al. PET using $^{18}$F-FDG in malignant lymphoma: a comparison with proliferative actitivity. *J Nucl Med* 1992;33:325–329.
4. Rege SD, Hoh CK, Glaspy JA, et al. Imaging of pulmonary mass lesions with whole-body PET and FDG. *Cancer* 1993;72:82–90.
5. Zanzi I, Vinciguerra V, Schulman P, et al. Evaluation of malignant lymphoma with FDG/PET studies [Abstract]. *Eur J Nucl Med* 1993;20:977.
6. Newman JS, Francis IR, Kaminski MS, Wahl RL. Imaging of lymphoma with PET with $^{18}$F-2-fluoro-2-deoxy-D-glucose: correlation with CT. *Radiology* 1994;190:111–116.
7. Shulkin BL, Mitchell DS, Ungar DR, et al. Neoplasms in a pediatric population: $^{18}$F-fluoro-2-deoxy-D-glucose PET studies. *Radiology* 1995;194:495–500.
8. Chaly T, Mattacchiere R, Velez JW, et al. A large scale manual production of $^{18}$F-FDG using a synthetic unit made of sterile disposable components and operated by a master slave manipulator. *Appl Radiat Isot* 1990;41:29–34.
9. Wahl RL, Zassadry K, Helvie M, et al. Metabolic monitoring using chemohormonotherapy using PET initial evaluation. *J Clin Oncol* 1993;11:2101–2111.
10. Zanzi I, Robeson W, Vinciguerra V, et al. Imaging of gastrointestinal neoplasms with PET [Abstract]. *Eur J Nucl Med* 1991;18:687.
11. Jochelson M, Mauch P, Balikian J, et al. The significance of the residual mediastinal mass in treated Hodgkin's disease. *J Clin Oncol* 1985;3:637–640.
12. Luker GD, Siegel MJ. Mediastinal Hodgkin's disease in children: response to therapy. *Radiology* 1993;189:737–740.
13. Anderson KC, Leonard RCF, Canellos GP, et al. High-dose gallium imaging in lymphoma. *Am J Med* 1983;75:327–331.
14. Gasparini MD, Balzarini L, Castellani MR, et al. Current role of gallium scan and magnetic resonance imaging in the management of mediastinal Hodgkin lymphoma. *Cancer* 1993;72:577–582.
15. Even-Sapir E, Bar-Shalom R, Israel O, et al. Single-photon emission computed tomography quantitation of gallium citrate uptake for the differentiation of lymphoma from benign hilar uptake. *J Clin Oncol* 1995;13:942–946.
16. Cohen M, Hill CA, Cangir A, Sullivan MP. Thymic rebound after treatment of childhood tumors. *Am J Radiology* 1980;135:151–156.
17. Peylan-Ramu N, Haddy TB, Jones E, et al. High frequency of benign mediastinal uptake of $^{67}$Ga after completion of chemotherapy in children with high-grade non-Hodgkin's lymphoma. *J Clin Oncol* 1989;7:1800–1806.
18. Chapman PE, Groshar D, Hooper HR, et al. Does gallium uptake in the pulmonary hila predict involvement by non-Hodgkin's lymphoma? *Nucl Med Commun* 1992;13:730–737.
19. Stomper PC, Cholewinski SP, Park J, et al. Abdominal staging of thoracic Hodgkin disease: CT lymphangiography- $^{67}$Ga scanning. *Radiology* 1993;187:381–386.
20. DiChiro G, DeLaPaz RL, Brooks RA, et al. Glucose utilization of cerebral gliomas measured by $^{18}$F-FDG and PET. *Neurol* 1982;32:1323–1329.
21. Patz EF, Goodman PC. PET imaging of the thorax. *Adv Chest Radiology* 1994;32:811–823.
22. Bares R, Galonska P, Dempke W, et al. Somatostatin receptor scintigraphy in malignant lymphoma: first results and comparison with glucose metabolism measured by PET. *Horm Metab Res Suppl* 1993;27:56–58.
23. Rettonbacher, Galvan G. Differentiation between residual cancer and thymic hyperplasia in malignant non-Hodgkin's lymphoma with somatostatin receptor scintigraphy. *Clin Nucl Med* 1994;19:64–65.
24. Harris EW, Rakow JI, Weiner M, Agress H. Thallium-201 scintigraphy for assessment of a gallium-67-avid mediastinal mass following therapy for Hodgkin's disease. *J Nucl Med* 1993;34:1326–1330.

# Scintigraphic Monitoring of Reticuloendothelial System in Patients with Type 1 Gaucher Disease on Enzyme Replacement Therapy

Mordechai Lorberboym, Gregory M. Pastores, Chun K. Kim, George Hermann, Neville Glajchen and Josef Machac

*Division of Nuclear Medicine, Department of Radiology, and Departments of Human Genetics, Pediatrics and Diagnostic Radiology, Mount Sinai School of Medicine, City University of New York, New York, New York*

The purpose of this study was to define the scintigraphic pattern of marrow replacement and changes in reticuloendothelial activity after enzyme replacement therapy in patients with Gaucher disease. **Methods:** Forty patients underwent baseline whole-body imaging with $^{99m}$Tc-sulfur colloid and evaluation of liver and spleen volume with CT or magnetic resonance imaging. Thirty-seven of the 40 patients were treated with enzyme replacement. Therapeutic responses of central and peripheral bone marrow and the changes in pulmonary uptake of $^{99m}$Tc-sulfur colloid were assessed visually at 1–4 yr after the start of therapy. Changes in liver and spleen volumes were analyzed quantitatively. The initial pattern of marrow involvement was correlated with disease severity (based on baseline blood counts and liver and spleen volumes). **Results:** Baseline studies revealed that 38 of 40 (95%) and 28 of 40 (70%) of the patients in this study had abnormal peripheral and central marrow activity, respectively. Twenty of 24 evaluable patients (83.3%) on therapy showed regression of peripheral bone marrow activity to a more proximal location in the lower extremities, increased ratio of pelvic/proximal femoral activity to distal activity or both. Fourteen of 19 treated patients (73.7%) with abnormal initial central marrow activity showed detectable improvement in central bone marrow activity as a result of therapy. In patients with initial lung uptake of $^{99m}$Tc-sulfur colloid, 91% showed complete resolution of the uptake after therapy. These changes in colloid uptake and distribution were associated with significant reductions in liver and spleen volumes and improvements in blood counts. **Conclusion:** Most patients with Gaucher disease demonstrate increased central bone marrow activity and regression of activity in peripheral bone marrow with enzyme replacement therapy. Additionally, the abnormal phagocytic pulmonary activity observed before therapy in many of the patients resolves.

**Key Words:** Gaucher disease; enzyme therapy; technetium-99m-sulfur colloid

**J Nucl Med 1997; 38:890–895**

Gaucher disease (GD) is an inborn error of glycosphingolipid metabolism due to deficiency of the lysosomal hydrolase, glucocerebrosidase. Clinically, three subtypes are delineated on the basis of the absence (Type 1) or presence and severity (acute Type 2 and subacute Type 3) of neurologic involvement. The primary features include progressive hepatosplenomegaly, skeletal disease and anemia and thrombocytopenia as a result of replacement of the bone marrow with lipid-laden macrophages ("Gaucher cells") (*1,2*). The peripheral spread of the Gaucher cell infiltrate is accompanied by progressive replacement of marrow adipocytes in the axial and appendicular skeleton. Enzyme replacement therapy using placenta-derived (alglucerase) or recombinant (imiglucerase) glucocerebrosidase eliminates most of the clinical manifestations (*3,4*).

We report our experience with reticuloendothelial system (RES) scintigraphy using $^{99m}$Tc-sulfur colloid (sulfur chloride)

Received May 15, 1996; revision accepted Oct. 8, 1996.

For correspondence or reprints contact: Mordechai Lorberboym, MD, Division of Nuclear Medicine, Box 1141, Mount Sinai Medical Center, One Gustave L. Levy Place, New York, NY 10029.

($^{99m}$Tc-SC) in patients suffering from Type 1 GD and the outcome of treatment with enzyme replacement over a period of 1–4 yr.

## MATERIALS AND METHODS

### Study Population

Forty consecutive patients, 18 males and 22 females, with Type 1 GD, ranging in age from 10 to 73 yr (mean, 40.6 ± 16.2 yr), were evaluated. All patients or their guardians gave informed consent. A detailed medical history was obtained from each patient. Patients who had a concurrent major medical disorder (e.g., cancer, cardiac disease or renal disease) were excluded from this study. Each patient had a physical examination and laboratory studies, including a complete blood count, serum chemistries and urinalysis. Long bone surveys and CT or magnetic resonance imaging (MRI) scans for liver and spleen volume were also obtained. The diagnosis of Type 1 GD was based on the marked deficiency of glucocerebrosidase activity in skin fibroblasts, peripheral blood leukocytes or both.

Fourteen of 40 patients (35%) underwent a total splenectomy before baseline studies. The mean age at splenectomy was 21.8 ± 11.6 yr (range, 7–38 yr).

Thirty-seven of 40 patients received alglucerase. The mean enzyme dose was 47.1 ± 11.1 units/kg of body weight every 2 wk (range, 30–60 units/kg). Treatment was administered over a mean period of 31.6 ± 11.5 mo (range, 11.5 ± 57.3 mo).

### Radionuclide Scintigraphy

Combined bone marrow and liver/spleen scintigraphy was performed 30 min after i.v. administration of $^{99m}$Tc-SC (10 mCi), using a wide-field-of-view gamma camera and a low-energy, all-purpose, parallel-hole collimator. Anterior and posterior sequential 5-min images of the whole body were obtained. Quality control of the radiopharmaceutical preparation was performed by thin-layer chromatography, and labeling efficiency was over 97%. There was no excess alumina in the preparation.

Visual analysis of central and peripheral bone marrow distribution and the pattern of pulmonary uptake of $^{99m}$Tc-SC were recorded before and after therapy. No follow-up scans were available for the three untreated patients. Two experienced nuclear medicine physicians interpreted and reviewed the studies separately. Disagreements were resolved by a consensus.

### Peripheral Bone Marrow Expansion

The distribution of bone marrow in the appendicular skeleton was assessed, with special attention to uptake in the proximal and distal femora and tibiae. Activity in the pelvis and proximal femora was compared to activity in the distal femora and tibiae.

### Central Bone Marrow Activity

Bone marrow activity in the sternum, lumbar spine and pelvis was evaluated using the following grading system (Fig. 1): Grade 0, absent activity in the sternum and absent or faint activity in the lumbar spine and pelvis; Grade 1, activity in the lumbar spine and

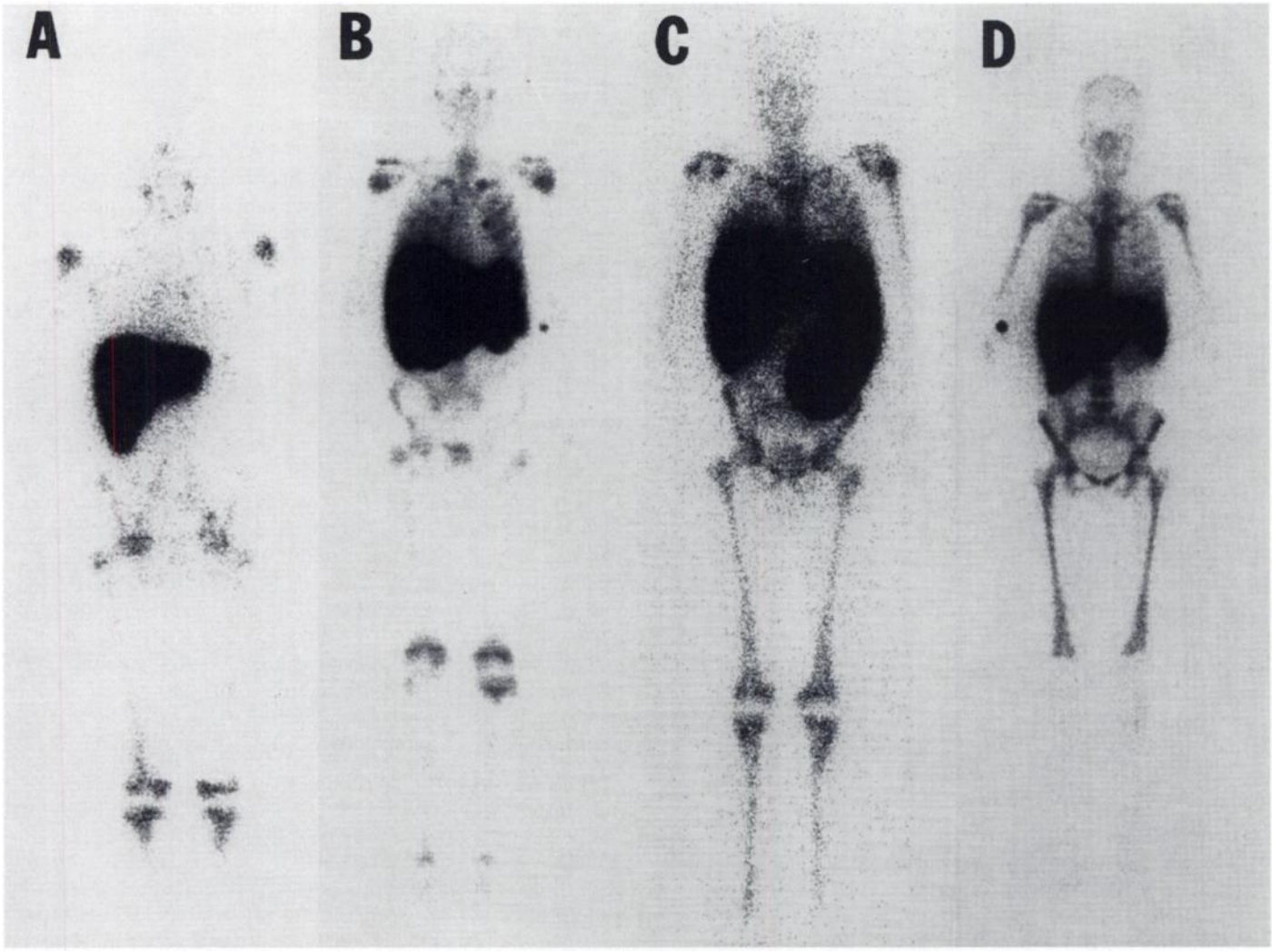


**FIGURE 1.** Four patients with GD at different stages of central bone marrow involvement (Grades 0–3, A–D, respectively). Note prominent activity at the shoulder joints even in Grade 0 uptake, despite marked depletion of bone marrow activity.

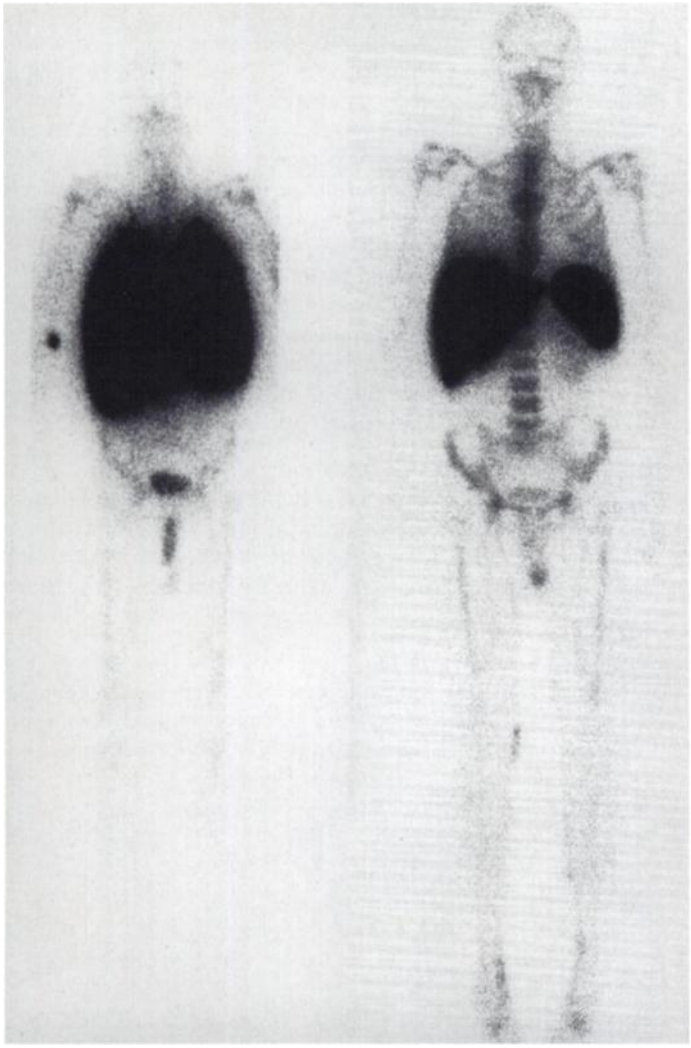

**FIGURE 2.** Effect of enzyme therapy in a patient with prominent lung uptake and diminished central marrow activity (left). After therapy, there is complete regression of pulmonary activity and repopulation of bone marrow (right). Note regression of hepatosplenomegaly.

pelvis less than that in the humeral heads and shoulder joints; Grade 2, activity in the lumbar spine and pelvis equal to that of the shoulders; and Grade 3, normal activity in the sternum, with activity in the lumbar spine and pelvis greater than that in the shoulders and visibly distinct rib activity. We used the shoulder joint as a reference point because it showed persistently high and constant activity over the years.

### Pulmonary Uptake

Visual analysis graded the lung uptake as absent (Grade 0), mild (Grade 1) or intense (Grade 2) using the following grading system: Grade 0, absent or background activity; Grade 1, more than background and equal to or less than bone marrow activity in the shoulders; and Grade 2, more than the activity in the shoulders. Special care was taken to separate true lung uptake from scattered liver activity.

Clinical lung involvement and pulmonary radiographic abnormalities were recorded for all patients.

### Imaging of the Liver and Spleen

Liver and spleen volumes were calculated from CT or MRI scans. CT scans were performed using 10-mm contiguous cuts to cover both the liver and spleen. Magnetic resonance (MR) images were obtained using T1-weighted images and two signal averages with respiratory compensation by 10-mm-thick sections without any interslice gap.

**TABLE 1**
Extent of Peripheral Bone Marrow Expansion in Patients with GD Before and After Therapy (n = 24)

| | Post-therapy | | |
|---|---|---|---|
| Pre-therapy | Regression* (n = 3) | Increased ratio† (n = 18) | No change‡ (n = 4) |
| Distal femora (n = 5) | | 2 | 3 |
| Proximal tibiae (n = 6) | 1 | 5 | |
| Mid-tibiae (n = 5) | 1 | 4 | |
| Distal tibiae (n = 7) | | 6 | 1 |
| Feet (n = 1) | 1§ | 1§ | |

*Proximal regression of bone marrow activity.
†Increased ratio of pelvic/femoral-to-distal activity.
‡No change in bone marrow distribution.
§This patient had regression of activity and increased proximal-to-distal ratio as well.

The CT/MR images were used to manually trace the borders of the liver and spleen. A region of interest cursor was then placed in the center of the traced area to define a region in square millimeters or centimeters. These values were then summed to give the volume of each organ in cubic centimeters.

The liver and spleen volumes were expressed as the fold increase over the predicted mean normal volume (i.e., 2.5% and 0.2% of body weight for liver and spleen, respectively). Hepatomegaly was defined as a liver volume $\geq$1.13 times the expected volume. Splenomegaly was defined as a splenic volume $\geq$2 times the expected volume.

### Statistical Analyses

The association between baseline bone marrow findings, hematological indices (hemoglobin and platelets) and organ volumes (liver and spleen) were analyzed using Spearman's correlation. The influence of the presence or absence of the spleen on the baseline bone marrow findings was evaluated using the unpaired Student's t-test. Test findings were compared before and after therapy using the paired Student's t-test for hemoglobin, liver and spleen volumes, the signed-rank test for platelet counts and the sign test for bone marrow findings.

## RESULTS

### Hematological Response

At baseline, anemia (Hg $\leq$ 12 g%) was noted in 25 patients (62.5%) [mean hemoglobin levels were 10.4 $\pm$ 1.0 g% (range, 8–11.6 g%)], including 9 of 14 (64.2%) splenectomized patients. Thrombocytopenia (platelet count $\leq$140,000 platelets per $mm^3$) was present in 20 (50%) patients [mean 78.4 $\pm$ 30.5 $\times$ 1000 platelets per $mm^3$ (range, 31–140,000 platelets per $mm^3$)]. None of the splenectomized patients had thrombocytopenia.

Patient responses on enzyme therapy varied widely. Nevertheless, there was a mean increase of 1.6 $\pm$ 2.2 g% in hemoglobin level ($p < 0.001$) and 36.6 $\pm$ 77.7 $\times$ 1000 platelets per $mm^3$ in platelet counts ($p < 0.002$) from baseline.

### Peripheral Bone Marrow Expansion

Before therapy, 38 of 40 (95%) patients had abnormal peripheral bone marrow expansion. Table 1 lists the distribution of peripheral bone marrow activity in 24 patients with follow-up data. There was a significant correlation between the pattern of bone marrow distribution at baseline and the degree of hepatosplenomegaly. There was a trend towards lower blood counts among patients with greater abnormalities in baseline bone marrow findings, although this did not achieve statistical

**TABLE 2**
Central Bone Marrow Distribution in Patients with GD (n = 40)

| | Post-therapy | | | | |
|---|---|---|---|---|---|
| Pre-therapy | Grade 0 (n = 2) | Grade 1 (n = 0) | Grade 2 (n = 6) | Grade 3 (n = 21) | No F/U (n = 11) |
| Grade 0 (n = 12) | 2 | | | 6 | 4 |
| Grade 1 (n = 9) | | | 3 | 3 | 3 |
| Grade 2 (n = 7) | | | 3 | 2 | 2 |
| Grade 3 (n = 12) | | | | 10 | 2 |

See text for grading system. F/U = follow-up.

significance ($p < 0.06$). Although not statistically significant, there was more extensive peripheral bone marrow expansion among splenectomized than among nonsplenectomized patients. Eighteen of 24 (75%) patients showed relative increase in bone marrow activity in the pelvis or proximal femora compared to distal marrow activity, whereas three patients showed visible regression of bone marrow to a more proximal location in the lower extremities (one of them belonged also to the previous category). Thus, 20 of 24 patients (83.3%) had detectable changes in peripheral bone marrow distribution.

### Central Bone Marrow Activity

Table 2 lists the changes in central bone marrow activity. Before therapy, 28 of 40 (70%) of the patients had mild-to-marked diminution in central bone marrow activity. There was no statistical difference in central bone marrow activity at baseline between splenectomized and nonsplenectomized patients. Fourteen of 19 treated patients (73.7%) with abnormal initial marrow activity and follow-up scans showed visible improvement in central bone marrow uptake of $^{99m}$Tc-SC after therapy ($p < 0.001$), whereas 5 patients (26.3%) showed no change, despite extraskeletal responses including improvements in blood counts and reduction of splenomegaly and/or hepatomegaly. Four of the five latter patients also showed no detectable regression or improvement in peripheral marrow expansion.

### Pulmonary Uptake

Twenty-nine of 40 patients (72.5%) had significant lung uptake of $^{99m}$Tc-SC on initial examination (Table 3). The degree of pulmonary uptake was correlated directly with the severity of central marrow activity and peripheral marrow expansion at baseline. Follow-up data were available for 22 treated patients; in 20 (91%), the follow-up scan showed complete regression of previously increased lung uptake with treatment ($p < 0.01$). The other two patients showed either persistent Grade 1 uptake or improvement from Grade 2 to Grade 1 uptake. Fourteen of 20 patients (70%) with resolution of pulmonary uptake also had concurrent improvement in central bone marrow activity (Fig. 2).

**TABLE 3**
Comparison of Lung Uptake Before and After Enzyme Therapy (n = 40)

| | Post-therapy | | | |
|---|---|---|---|---|
| Pre-therapy | Grade 0 (n = 29) | Grade 1 (n = 2) | Grade 2 (n = 0) | No F/U (n = 9) |
| Grade 0 (n = 11) | 9 | | | 2 |
| Grade 1 (n = 10) | 8 | 1 | | 1 |
| Grade 2 (n = 19) | 12 | 1 | | 6 |

See text for grading system. F/U = follow-up.

Of the remaining 11 patients with no lung uptake, 9 showed no changes on therapy and 2 had no follow-up. Only one patient had clinical lung disease manifested by cyanosis and dyspnea on exertion. This patient had evidence of interstitial lung disease on radiographs. The initial colloid scan, which was obtained 2 mo after high-dose therapy, showed no lung uptake. No changes were observed on the follow-up scan performed 36 mo later.

### Liver and Spleen Volume

At baseline, marked splenomegaly (mean volume, 17.4 ± 14.2 times normal; range, 3.6–51 times normal) appeared in 26 patients (65%). Hepatomegaly was present in 36 of 40 patients (90%); the mean liver volume was 2.2 ± 0.86 times normal (range, 1.13–4.34 times normal). Liver dysfunction (based on elevated serum amino transferase levels) appeared in 12 of 40 (30%) of patients.

Enzyme therapy resulted in a mean decrease in liver volume of 24.5% ± 20.9% (range, +19.4 to −82.5%) from baseline ($p < 0.001$). Spleen volume diminished by 39.9% ± 30.4% ($p < 0.001$).

## DISCUSSION

GD is an autosomal recessive disorder of glycosphingolipid metabolism. Although prevalent among Ashkenazi Jews, in whom carrier frequency is approximately 1 in 18, it has been described in all other ethnic groups. Although the disease is clinically characterized by multisystemic involvement, the skeletal manifestations are the most debilitating and disabling (*1*). The accumulation of unmetabolized glucocerebroside in bone marrow macrophages leads to replacement of the hematopoietic tissue and skeletal involvement, resulting in frequent fractures, episodic bone pain, osteopenia and osteonecrosis (*5*). The most typical change is the club-shaped (Erlenmeyer flask) deformity of the distal femora. Similar changes may be seen in the proximal tibiae (*2*).

Before enzyme replacement, the management of symptomatic patients was primarily palliative, with blood transfusions, splenectomy or both (for severely anemic patients) and with orthopedic interventions. Bone marrow transplantation has also been tried, and some regression of radiological abnormalities and clearing of pulmonary infiltrates has been reported in one patient (*5*). The development of macrophage-targeted human placentally derived and recombinant glucocerebrosidase provided an opportunity to evaluate the long-term hematological and skeletal responses to enzyme replacement therapy (*3,6*).

Knowledge of the natural evolution of bone marrow distribution in unaffected individuals is essential for proper evaluation of the abnormalities observed in patients with GD. Newborns have a wide distribution of cellular red marrow in the bones of their appendicular and axial skeleton (*7*). The change from peripheral red to peripheral yellow marrow occurs in the first decade of life and follows a predictable sequence (*8*). Marrow conversion proceeds from distal to proximal sites, with distal bones being converted more rapidly than proximal bones. The process continues until age 25, when most of the red bone marrow is retained in the vertebrae, sternum, ribs, pelvis, skull and proximal shafts of the femora and humeri. In situations of stress to the bone marrow, such as chronic anemia and chronic heart failure, and in marrow replacement disorders, such as GD, the yellow marrow often changes to red marrow. The spine and flat bones respond more quickly than other sites, followed by the proximal extremities and extending distally, the reverse of

the physiological marrow conversion. The colonization of extramedullary sites may occur by bone marrow-derived stem cells (*9*).

No clinical or biochemical predictors have been identified for the rate of progression or future severity of the disease process, and osseous findings on plain radiographs do not always reflect the extent of visceral disease or the total burden of Gaucher cells within the marrow and, therefore, cannot be used to follow the progress of the disease with confidence.

Dual-energy CT and MRI techniques can document an abnormally low spinal bone marrow fat content (*10–12*). Quantitative CT has shown that GD is accompanied by a generalized decrease in trabecular bone density. There is marked depression of marrow fat content due to infiltration of the bone marrow by Gaucher cells. However, the extent of fatty marrow replacement in the vertebrae does not correlate well with the clinical severity of the disease. This technique measures fat content in vertebrae without regard to replacement of hematopoietic marrow. MR images show intense signal in normal bone marrow because of the high fat content, whereas the most consistent MR finding in patients with GD is the dramatic reduction in marrow signal due to deposits of glucocerebroside within the marrow (*13*).

Several radiopharmaceuticals have been used in evaluating GD. Xenon-133 has been used on the assumption that deposits of Gaucher cells will alter the cellular composition of the bone marrow and thus alter tracer uptake and washout pattern. In one study, simultaneous imaging was obtained during washin and washout phases over the knees and lungs (*14*). Xenon uptake around the knees increased as the fat content of the femora and spine decreased. On the other hand, $^{52}$Fe scans showed increased extramedullary erythropoiesis in the liver and spleen (*15*). Technetium-99m-MDP (methylene diphosphonate) bone imaging has been used during acute bone crises to detect infarcts (*16*). However, the pattern of $^{99m}$Tc-MDP uptake is variable and usually does not reflect the severity of bone loss or bone resorption as assessed by CT and $^{99m}$Tc-SC (*1*).

The reports on imaging of the RES with colloids are scant (*1,17,18*). Several patterns of abnormal uptake have been described (*1*). In these studies, increased uptake in the long bones of the lower extremities appeared in the early stages of marrow expansion, whereas the most severely involved patients showed an almost total absence of $^{99m}$Tc-SC uptake. We found a significant correlation between the extent of peripheral bone marrow expansion and the severity of hepatosplenomegaly, suggesting that bone marrow scintigraphy may be helpful in monitoring the systemic burden of the disease. The absence of a statistically significant correlation between the baseline blood counts and severity of initial bone marrow findings may be attributed to the inclusion of splenectomized patients (with normal blood counts but severe baseline bone marrow changes) with nonsplenectomized patients (with abnormal blood counts). On therapy, 83.3% of patients showed detectable proximal regression of peripheral activity after therapy, indicating that this parameter may be useful in a long-term follow-up.

Review of the literature provided no methodical assessment of central bone marrow activity. Quantitative analysis of bone marrow redistribution was difficult because of the overlying activity from the liver or spleen in the central skeleton and because most of the pre-therapy scans were analog images. However, we noted significant depletion in central bone marrow activity in 70% of patients before therapy and increased central marrow uptake in 73.7% of patients after therapy. The absence of bone marrow changes in five patients on therapy may reflect the advanced stage of their disease; four patients (including two after splenectomy) had undergone hip replacement, and two other patients had severe bone disease (i.e., avascular necrosis) and had a partial splenectomy before therapy.

Some might argue that increased central marrow activity is secondary to colloid shift from the liver and spleen subsequent to reduction in organ volume after successful therapy. However, a colloid shift alone should not alter the ratio between central and peripheral activity or between proximal and distal activity as observed in most of our patients. In fact, no significant difference was found in central marrow activity at baseline between splenectomized and nonsplenectomized patients. Furthermore, the associated regression of pulmonary phagocytic activity in most patients also implies that repopulation of the RES in the central skeleton is most likely independent of liver and spleen volumes. Although not quantitative, this parameter, in conjunction with peripheral marrow changes and CT/MRI findings in the spine, seems to be a good indicator of the bone marrow response to therapy in patients with GD.

Pulmonary infiltrates or respiratory symptoms are uncommon in GD (*5*). The incidence of increased lung uptake of $^{99m}$Tc-SC in liver and spleen studies is reported to be 1.6–8%, predominantly in patients with metastatic disease, myelofibrosis, cirrhosis, infection, histiocytosis X, amyloidosis and mucopolysaccharidosis type II (Hunter disease) (*19–21*). In Hunter disease, increased lung uptake may be present for years and often increases in intensity as the disease progresses. Animal studies show that macrophages migrate from bone marrow, liver and spleen to the lungs and are trapped in the pulmonary capillary bed. The macrophages retain their ability to phagocytize intravascular colloid after migration (*20*). In our study, a striking percentage of patients (91%) showed significant regression of pulmonary colloid uptake after therapy, accompanied by central bone marrow repopulation in 70%. However, the resolution of pulmonary uptake may also occur independently of central or peripheral bone marrow repopulation and may reflect changes in pulmonary macrophage function or number with treatment. These findings may indicate that the basic disease process of macrophage migration is receding.

## CONCLUSION

Sequential radiocolloid images in patients with GD on therapy are helpful in demonstrating the changes in bone marrow and pulmonary uptake associated with improvements in hematological parameters and reduction of hepatosplenomegaly. Further studies are required to assess whether long-term enzyme therapy will result in complete regression of scintigraphic RES abnormalities.

## ACKNOWLEDGMENTS

We thank Alex Pechtchanski, Binu Chacko and Pamela Lenz, MS, for their research assistance. We also thank Dr. Elmer C. San Pedro and Ms. Maria Dacosta, CNMT, for their assistance in retrieving the scintigraphic images. This work was supported in part by the National Institutes of Health, including grant 5 M01 RR00071 for the Mount Sinai General Clinical Research Center from the National Center for Research Resources and grant 5 P30 HD28822 for the Mount Sinai Child Health Research Center. G.M. Pastores is the recipient of a Minority Clinical Associate Physician Award (5 M01-RR00071) from the National Institutes of Health.

## REFERENCES

1. Hermann G, Goldblatt J, Levy RN, Goldsmith SJ, Desnick RJ, Grabowski GA. Gaucher's disease type 1: assessment of bone involvement by CT and scintigraphy. *Am J Roentgenol* 1986;147:943–948.

2. Rourke JA, Heslin DJ. Gaucher's disease. *Am J Roentgenol* 1965;94:621–630.
3. Barton NW, Furbish FS, Murray GJ, Garfield M, Brady RO. Therapeutic response to intravenous infusions of glucocerebrosidase in a patient with Gaucher disease. *Proc Natl Acad Sci USA* 1990;87:1913–1916.
4. Grabowski GA, Barton NA, Pastores G, et al. Enzyme therapy in type 1 Gaucher disease: comparative efficacy of mannose-terminated glucocerebrosidase from natural and recombinant sources. *Ann Intern Med* 1995;122:33–39.
5. Starer F, Sargent JD, Hobbs JR. Regression of the radiological changes of Gaucher's disease following bone marrow transplantation. *Br J Radiol* 1987;60:1189–1195.
6. Parker RI, Barton NW, Read EJ, Brady RO. Hematologic improvement in a patient with Gaucher disease on long-term enzyme replacement therapy: evidence for decreased splenic sequestration and improved red blood cell survival. *Am J Hematol* 1991;38:130–137.
7. Ruzal-Shapiro C, Berdon WE, Cohen MD, Abramson SJ. MR imaging of diffuse bone marrow replacement in pediatric patients with cancer. *Radiology* 1991;181:587–589.
8. Kricon ME. Red-yellow marrow conversion: its effect on the location of some solitary bone lesions. *Skel Radiol* 1985;14:10–19.
9. Wang JC, Tobin MS. Mechanisms of extramedullary haematopoiesis in rabbits with saponin-induced myelofibrosis and myeloid metaplasia. *Br J Haematol* 1982;51:277–284.
10. Rosenthal DI, Mayo-Smith W, Goodsitt MM, Doppelt S, Mankin HJ. Bone and bone marrow changes in Gaucher disease: evaluation with quantitative CT. *Radiology* 1989;170:143–146.
11. Rosenthal DI, Barton NW, McKusick KA, et al. Quantitative imaging of Gaucher disease. *Radiology* 1992;185:841–845.
12. Cremin BJ, Davey H, Goldblatt J. Skeletal complications of type I Gaucher disease: the magnetic resonance features. *Clin Cardiol* 1990;41:244–247.
13. Lanir A, Hadar H, Cohen I, Tal Y, Benmair J, Schreiber R, Clouse ME. Gaucher disease: assessment with MR imaging. *Radiology* 1986;161:239–244.
14. Castronovo FP Jr, McKusick KA, Doppelt SH, Barton NW. Radiopharmacology of inhaled $^{133}$Xe in skeletal sites containing deposits of Gaucher cells. *Nucl Med Biol* 1993;20:707–714.
15. Dokal IS, Deenmamode M, Lewis SM. Radioisotope studies in monitoring of Gaucher's disease and its treatment. *Clin Lab Haematol* 1989;11:91–96.
16. Katz K, Mechlis-Frish S, Cohen IJ, Horev G, Zaizov R, Lubin E. Bone scans in the diagnosis of bone crisis in patients who have Gaucher disease. *J Bone Joint Surg* 1991;73:513–517.
17. Israel O, Jerushalmi J, Front D. Scintigraphic findings in Gaucher's disease. *J Nucl Med* 1986:27;1557–1563.
18. Cheng TH, Holman BL. Radionuclide assessment of Gaucher's disease. *J Nucl Med* 1978;19:1333–1336.
19. Klingensmith WC III, Tsan MF, Wagner, HN Jr. Factors affecting the uptake of $^{99m}$Tc-sulfur colloid by the lung and kidney. *J Nucl Med* 1976;17:681–684.
20. Stadalnik RC. Diffuse lung uptake of Tc-99m-sulfur colloid. *Semin Nucl Med* 1980;10:106–107.
21. Polga JP, Holsten G, Spencer RP. Radiocolloid redistribution and multiple splenic infarcts in myelofibrosis. *Clin Nucl Med* 1983;8:335–336.

# Extracorporeal Whole-Blood Immunoadsorption Enhances Radioimmunotargeting of Iodine-125-Labeled BR96-Biotin Monoclonal Antibody

Michael Garkavij, Jan Tennvall, Sven-Erik Strand, Hans-Olov Sjögren, Chen JianQing, Rune Nilsson and Martin Isaksson
*Departments of Oncology, Radiation Physics and Immunology, Lund University, Lund, Sweden*

This study investigates the efficacy of tumor radioimmunotargeting with $^{125}$I-labeled BR96-biotin monoclonal antibody using a new method, whole-blood immunoadsorption (WBIA), based on direct adsorption of unbound monoclonal antibody (MAb) from blood without preceding separation of plasma. **Methods:** Highly tumor-reactive, internalizing, chimeric BR96 MAb of isotype IgG1 binds to a tumor-associated Lewis-type ($Le^Y$) cell surface antigen. Forty-six Brown Norwegian male rats were inoculated intramuscularly and beneath the liver or kidney capsule with syngeneic rat colon carcinoma BN7005, expressing Lewis-type antigen, and investigated. The rats were injected intravenously with 3.5–4.5 MBq $^{125}$I-labeled BR96-biotin. Twenty of the rats underwent WBIA starting 5 or 12 hr after injection. About six blood volumes were passed through an avidin-gel adsorption column during 2 hr. **Results:** By using WBIA, whole-body radioactivity was reduced by 50%, and plasma activity by 85%. Both directly after completion of WBIA and 33 hr later, the activity uptake in tumors manifested only a nonsignificant decrease as compared with corresponding controls ($p > 0.05$) and had approximately similar time-activity curves. Uptake ratios for tumor (T):bone marrow, T:liver, T:kidney and T:lung were enhanced 2.3- to 3.5-fold in all three tumor models, as compared with controls. The ratio of liver tumor to bone marrow was improved from 10:1 to 30:1. **Conclusion:** This new method of WBIA yields significantly improved radioimmunotargeting of highly tumor-reactive, internalizing MAb BR96.

**Key Words:** tumor; rat; radioimmunotargeting; MAb BR96; immunoadsorption

**J Nucl Med 1997; 38:895–901**

Received Feb. 22, 1996; revision accepted Sep. 4, 1996.
For correspondence or reprints contact: Michael Garkavij, MD, Department of Oncology, Lund University Hospital, S-221 85, Lund, Sweden.

Recently published results (*1,2*) concerning monoclonal antibody immunoconjugate BR96-doxorubicin (DOX) have generated a wave of enthusiasm among researchers and clinicians working with monoclonal antibodies (MAb) for cancer therapy (*3*). BR96 has high tumor selectivity, can rapidly internalize, has a direct cytotoxic effect on antigen-positive tumor cells and mediates both ADCC and CDC (*4*). The chimeric version of BR96 has the same properties as the native MAb but an even stronger antitumoral effect (*5,6*). Immunological studies have demonstrated that BR96 binds to differentiated epithelial cells of gastrointestinal tract and to a majority (>75%) of human carcinomas of breast, lung, ovary and gastrointestinal tract, expressing this antigen (*7*). Trail et al. (*1*) showed BR96-DOX to cure 94% of athymic rats with subcutaneous human lung carcinoma, even though these naked rats, like humans and in contrast to mice, expressed the BR96-target antigen in normal tissues although to a lesser extent than humans. On the other hand, several clinicians have shown some skepticism, pointing out that the preclinical data regarding MAb-based tumor targeting have not always been confirmed clinically (*8,9*). One argument is that studies of human tumors growing in immunocompromised animals are not ideal for predicting antitumoral activity in the clinical setting. Moreover, in the case of drug conjugates that act stoichiometrically, a crucial factor is antigen density that should be very high to allow the intracellular localization of a sufficient number of cytotoxic molecules (*9*). When antigen expression is low or heterogeneous, as is usually the case in the clinical situation, conjugates with beta-emitting radionuclides may be more effective (*10*).

Extracorporeal immunoadsorption (ECIA) is a new method for selective removal of circulating radiolabeled monoclonal